

Investigation of electrical, structural and thermal stability properties of cubic $(\text{Bi}_2\text{O}_3)_{1-x-y}(\text{Dy}_2\text{O}_3)_x(\text{Ho}_2\text{O}_3)_y$ ternary system

Refik Kayali^{1,*}, Murivet Kasikci¹, Semra Durmus², Mehmet Ari²

¹Department of Physics, Science-Literature Faculty, Nigde University, Nigde, Turkey

²Department of Physics, Science-Literature Faculty, Erciyes University, Kayseri, Turkey

* Corresponding author. Tel: +90 388 225 4069, Fax: +90 388 225 0180, E-mail: refikkayali@nigde.edu.tr

Abstract: In the scope of this work, $(\text{Bi}_2\text{O}_3)_{1-x-y}(\text{Dy}_2\text{O}_3)_x(\text{Ho}_2\text{O}_3)_y$ ternary system ($x=1,3,5,7,9,11$ mol % and $y=11,9,7,5,3,1$ mol %, dopant concentrations) sample materials were developed using solid state reaction method sintering each of them at 650, 700, 750, 800 °C for 48 hours. Structural, electrical and thermal properties of these samples which are candidate of electrolyte for solid oxide fuel cells (SOFCs) have been evaluated by means of XRD, four-probe method, and TGA / DTA. XRD measurements showed that except the samples annealed at 650 °C, all the other samples have stabilized δ - Bi_2O_3 phase. It was seen that duration of sintering time and temperature was rather effective on the formation of the stabilized sample materials and their other properties, such as electrical and structural properties. It was seen that the electrical conductivities of all the examples developed sintering at 700, 750 and 800 °C for 48 hours increases with the increasing temperature having numerical values varying in the range of $7,65 \times 10^{-2} \Omega \cdot \text{cm}^{-1}$ - $6,11 \times 10^{-1} \Omega \cdot \text{cm}^{-1}$. Activation energy of the sample A6 was calculated and it was found 0.97 eV. On the other hand, the main purpose of this study is to find an electrolyte which does not have any degradation in its properties with time; this maybe caused either interaction between the different electrochemical cell materials or by instability of the ionic conductor under operation conditions. During the heating/cooling process, the four-point probe conductivity measurements have been performed. The hysteresis curve was obtained for this sample due to time interval difference of heating/cooling processes. It was observed that there is no gradation in the structure of the sample.

Keywords: Electrolyte, Solid state reaction, Fuel cell, Electrical conductivity, XRD, Four- probe point method

1. Introduction

Recently, it has been known that bismuth oxide based and doped with the other two ceramic oxides are ternary materials with the properties showing promise of utility in SOFC's [1-7]. In addition, the need to develop oxide ion conductive materials with high conductivity and desired structure stability at low temperature directs most of the research toward solid oxide electrolyte materials. Among these electrolyte materials, Bi_2O_3 - based solid oxide electrolyte materials with δ -phase fcc fluorite type crystal structure are of interest for use in solid oxide fuel cell (SOFC) due to their high oxide ion conductivity [8,9]. The fluorite type phase of pure Bi_2O_3 , known as the most highly conductive oxide-ion conductor, has a conductivity of about 1 Scm^{-1} at 750 °C. But, δ -phase Bi_2O_3 is stable only between 730 °C and 825 °C and cannot be quenched to room temperature [10]. However, the δ -phase can be obtained at room temperature by doping with some transition metal (Nb, Ta, V and W) and rare earth (Sm-Lu). It is also possible to use combination of oxides, so called double doping, to obtain the δ fluorite type phase. Fluorite type δ -phase materials displays very high oxide ion conductivity which is attributed to the highly polarisable Bi^{3+} cations and highly disordered structure of sublattice [11-15]. Structural and conductive properties of a solid material during the various temperature ranges determine its suitability as an electrolyte in the practical use. If an electrolyte material has a high conductive behavior over a long period of time at reasonably low temperature, it is possible to use at operation of a SOFC. Many researchers were reported that the fluorite type δ -phase Bi_2O_3 cannot be stabilized [11-13]. Some these kinds of materials had completely transformed into mixture phases after annealing for long time period. In addition, the conductivity decay can also occur for the fluorite type materials without changing its structure. The rate of conductivity decay is dependent on annealing temperature, long ordering oxide-ion sublattice and amount of doped cations.

2. Experimental

2.1. Sample preparation

We have tried to stabilize the fluorite type δ -phase in the ternary system $(\text{Bi}_2\text{O}_3)_{1-x-y}(\text{Dy}_2\text{O}_3)_x(\text{Ho}_2\text{O}_3)_y$. As a result, we could obtain a stabilized δ -phase in limited compositional range of x and y .

The desired proportions of the samples were accurately weighed and thoroughly mixed. The mixture was heated in an alumina crucible at 750 °C for 10 h and quenched to room temperature by air stream. Next, the samples were examined by XRD using $\text{CuK}\alpha$ radiation. Then, the prepared pellets were annealed at 650, 700, 750 and 800 °C for 48 h followed by air quenching. The same heat treatment was repeated several times in order to get its equilibrium state, after the conductivity measurements were performed in air. Finally, thermal behavior of the samples was taken the differential thermal analysis (DTA) measurements in order to find out whether any phase transition exists or not, after each measurement.

2.2. XRD measurements

Powder XRD measurements is carried out by using Bruker AXS D8 Advance type diffractometer with an interval $2\Theta = 10^\circ\text{--}90^\circ$, scanning 0,002°/min, and $\text{Cu-K}\alpha$ radiation for the determination of the crystal structure of the samples at room temperature. These measurements were repeated for the powders of the samples obtained after every sintering process. Then, Diffrac Plus Eva packet program was used to analyze the unit lattice cell parameters (a , b , c , α , β , γ), Miller indexes, and the distance between the layers, d . On the other hand, Win-Index Professional Powder Indexing packet program was used for the indexing of the diffraction peaks in the powder patterns of the samples.

2.3. Electrical measurements

Conductivity of the samples was measured using four-point probe method. The pellets of the samples with 13 mm diameter and 2 mm thick were obtained by using a conventional press and then the pellets were being air-quenched after sintering. All of the measurements in this work were carried out by means of Data Acquisition Control System associated with a PC, interface card IEEE-488.2, multimeter with scanning card (Keithley 2700, 7700-2), programmable power supply (Keithley 2400), and computer program written for this purpose. These measurements were repeated for several times because of the electrical conductivity measurements performed during the first heating process are not enough to represent the complete electrical behavior of the samples.

2.4. TG/DTA measurements

The thermal behavior of the annealed materials was investigated by DTA/TG by means of DIAMOND TG/DTA-PERKIN ALMER Marck system. The samples whose masses are about 20-50 mg were heated at 200 °C min^{-1} in an alumina crucible and cooled quickly to room temperature under a stream of air.

3. Results and discussion

3.1. XRD measurement results

Figure 1 shows the comparisons of the XRD spectra of the samples annealed at 650 °C for 48 hours. As seen from this figure, all the samples do not have completely monoclinic- α phase, but some of them have also δ -phase. As a result, the samples prepared at this temperature have a mixed phase and the formation of the δ -phase also exhibits at this stage.

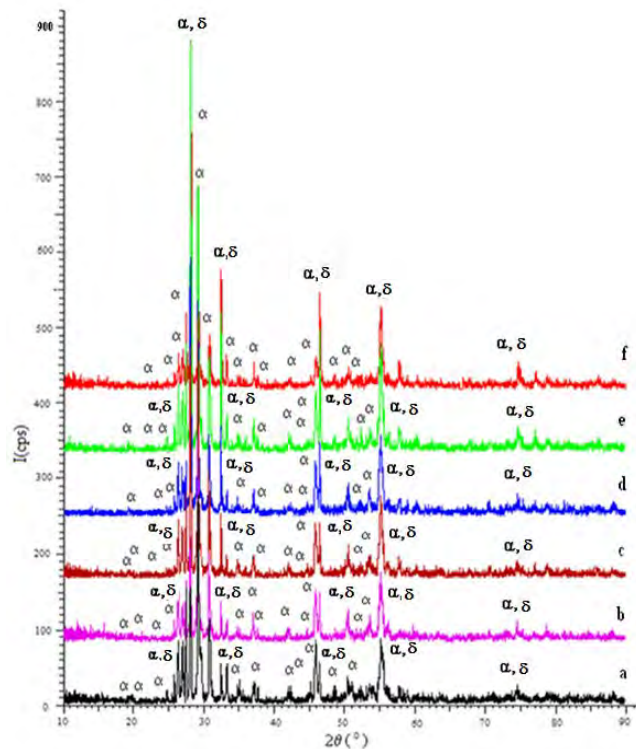


Fig.1. Comparisons of the XRD spectra of the samples annealed at 650 °C and for 48 hours and having $\alpha+\delta$ - Bi_2O_3 phase (a) A1, (b) A2, (c) A3, (d) A4, (e) A5 and (f) A6

Figure 2 shows the comparisons of the XRD spectra of the samples annealed at 750 °C for 48 hours. From this figure, it is observed that all the samples except A1 have only δ -phase. Two peaks at the right and left side of the most intensive peak of the sample A1 are seen and they are belonging to the α -phase. No significant modification of the intensity of the XRD pattern can be detected, which means that the δ -phase of the samples has not been decomposed into the other low conductivity phases by changing amount of the doped materials.

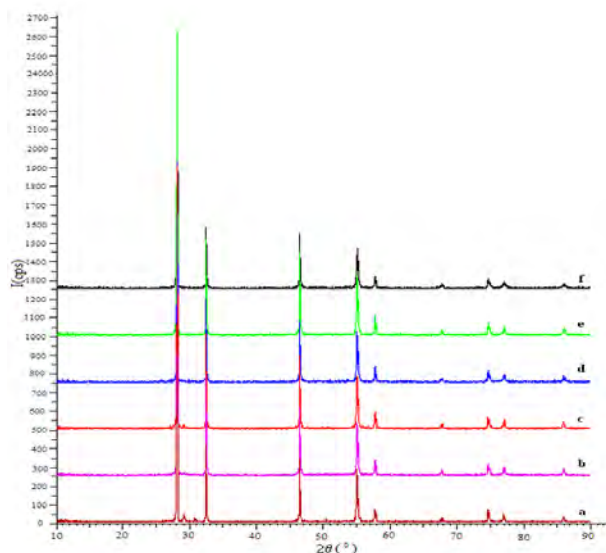


Fig. 2. Comparisons of the XRD spectra of the samples annealed at 750 °C and for 48 hours and having fcc δ - Bi_2O_3 phase (a) A1, (b) A2, (c) A3, (d) A4, (e) A5 ve (f) A6

Also, there is no transformation of the quenched δ -phase is evidenced on the XRD patterns. The fluorite type δ -phase is obtained at the end of the process. The first generated δ -phase has

been kept stable during the electrical measurement annealed at 700, 750, 800 °C for all the samples.

Summary of the observed phases from XRD measurements of the $(\text{Bi}_2\text{O}_3)_{1-x-y}(\text{Ho}_2\text{O}_3)_x(\text{Dy}_2\text{O}_3)_y$ ternary-systems with different dopant ratios and developed at different temperatures mentioned above is given in Table 1. As seen from this table, all the samples except the samples annealed at 650 °C have stable fcc δ -phase.

Table 1. Observed phases for $(\text{Bi}_2\text{O}_3)_{1-x-y}(\text{Ho}_2\text{O}_3)_x(\text{Dy}_2\text{O}_3)_y$ ternary-systems with different dopant ratios and developed at different temperatures

Synthesing temperature (°C)	Synthesing time (hour)	$(\text{Ho}_2\text{O}_3)_x(\text{Dy}_2\text{O}_3)_y(\text{Bi}_2\text{O}_3)_{1-x-y}$ ($x,y = \text{mol } \%$)					
		x=1 y=11	x=3 y=9	x=5 y=7	x=7 y=5	x=9 y=3	x=11 y=1
650	48	$\alpha + \delta$	$\alpha + \delta$	$\alpha + \delta$	$\alpha + \delta$	$\alpha + \delta$	$\alpha + \delta$
700	48	δ	δ	δ	δ	δ	Δ
750	48	δ	δ	δ	δ	δ	Δ
800	48	δ	δ	δ	δ	δ	Δ

3.2. Electrical conductivity measurements

The conductivity measurements were performed on the samples $(\text{Bi}_2\text{O}_3)_{1-x-y}(\text{Dy}_2\text{O}_3)_x(\text{Ho}_2\text{O}_3)_y$ ternary system ($x=1,3,5,7,9,11$ mol % and $y=11,9,7,5,3,1$ mol %). Conductivity measurements were only carried out up to 850 °C in order to ensure that melting does not occur. In this report, we have presented only the electrical measurements of the samples developed at 750 °C, since it has the best conductivity. The conductivity of this sample is $0.6 (\Omega \cdot \text{cm})^{-1}$ placing it among the most highly conductive materials known.

Figure 3 shows the graphics of the conductivity of the samples versus to $1000/T$ K. As seen from this figure, all the curves are similar with each other. It is the expected result since all of them have stable fcc δ -phase. These results were supported by the XRD patterns of the samples which have been given in Fig.3 too.

The Ho_2O_3 rich samples show higher electrical conductivity than the Dy_2O_3 rich materials. The conductivity results show that an intermediate fast changing conductivity region separated by linear evolution zone. The sharp rise of the conductivity is indication of an order-disorder transition.

Increase in the conductivity of the materials with increasing amount of Ho_2O_3 is attributed to the increase in the proportion of highly polarisable cations and in the number of oxide ion vacancies. It can be noticed that the conductivity slightly increases with increasing the Ho_2O_3 proportion, reaching highest values $0.6 (\Omega \cdot \text{cm})^{-1}$ for $x=11$ an $y=1$ %mol (A6). This can simply be explained that can be attributed to the increase in the concentration of vacancies by the Ho cations located on the host sub-lattice, which are available for oxide ion migration. The distribution of vacancies affects the long range migration of oxide ions and therefore the conductivity increases. Since dopant cations and oxide ion vacancies have negative and positive charges, attractions between them are likely to be mainly responsible for the high activation energy. As a result, it can be said that an electrical conductivity rise has been observed for all samples when the proportion of the Ho^{3+} cation is increased.

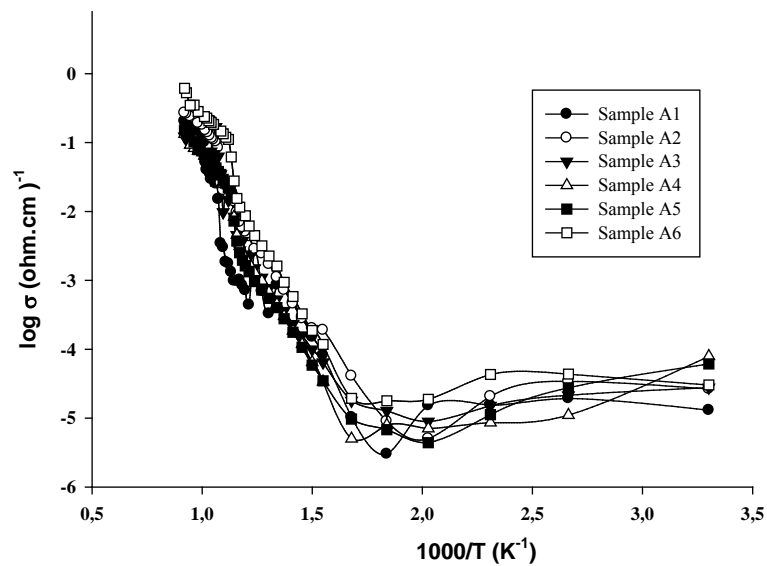


Fig. 3. Oxygen conductivity, as a function of temperature, for the samples A1, A2, A3, A4, A5, A6 obtained at 750 °C for 48 hours

Figure 4 shows the graphic of the conductivity of the sample A6 versus to 1000/T K at different annealing temperatures. As seen from this figure, two distinct regions observed on the curves corresponding to an order-disorder δ -phase transition which exhibits similar activation energy at these two regions. The characteristics of the conductivity curves are similar for all the samples. The conductivity values slightly increase with decreasing the annealing temperature especially at high temperature region.

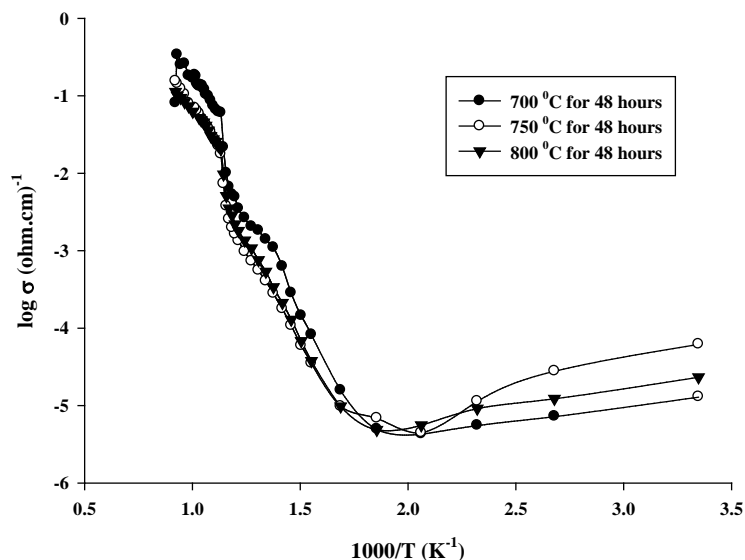


Fig. 4. Oxygen conductivity, as a function of temperature, for the sample A6

Activation energies of the samples can be obtained from the Arrhenius equation. As mentioned previously two distinct regions are observed for all samples corresponding to an order-disorder δ -phase transition which exhibits similar activation energy at these two regions. Activation energy calculated for sample A6 corresponding to the high temperature region is found 0.97 eV. And also, the conductivity results are in good agreement with these

already revealed by XRD and DTA/TG measurements. The samples which exhibit the lowest activation energy is associated the structure characterized by the fluorite type fcc lattice is likely responsible for opening of migration pathways for the oxide ions, and consequently to a decreasing of the activation energy.

The main purpose of this study is to find an electrolyte which does not have any degradation in its properties with time; this maybe caused either interaction between different electrochemical cell materials or by instability of the ionic conductor under operation conditions. So this sample has been firstly heated from room temperature to 650, 700, 750 and 800 °C in 48 hours and cooled from this temperature to room temperature in the same time. After this process, the four-point probe conductivity measurements have been performed.

Figure 5 shows the hysteresis curve obtained for the sample A6. This sample has been firstly heated from room temperature to 800 °C in 2 hours and cooled from this temperature to room temperature within the 4 hour s. During this process, the four-point probe conductivity measurements have been performed. The hysteresis curve was occurred for this sample due to time interval difference of heating/cooling processes. From this figure, the slopes of these curves nearly are the same. It means that there is no gradation in the physical and chemical properties of this sample after applying the operation condition.

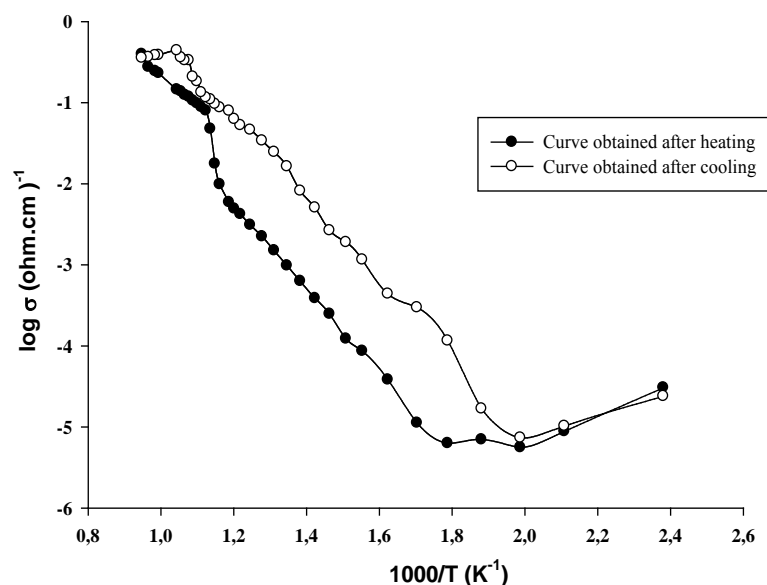


Fig. 5. Conductivity hysteresis curve obtained for the sample A6 obtained approximately 5 hours being heated from room temperature to 800 °C and cooled to room temperature

TG/DTA measurements of the samples have been carried out after the conductivity measurements of the samples using the same pellets. In figure 6, TG/DTA graphics of the sample A6 annealed at 750 °C and for 48 hours are given. From this figure, a wide range of exothermic peak is seen in a temperature range between 325-415 °C for A6 sample in DTA curve. Similar variation is seen between the same temperature ranges in TGA curve whose slope is changing during heating treatment. In this case, this peak results from the order/disorder transformation in the structure of the sample rather than the phase transformation. During the cooling process, there are no exothermic peak and slope changes because of long cooling time interval. This transformation is seen in the conductivity graphics of the same sample and its hysteresis curve (Fig. 5) too.

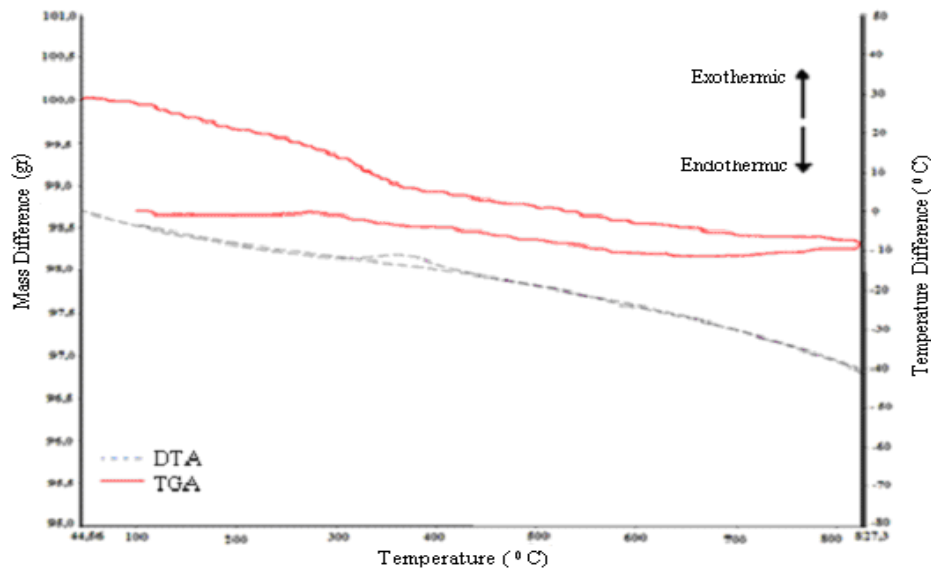


Fig. 6. TG/DTA graphics of sample A6 developed at 750 °C and for 48 hours

4. Conclusion

In this work, data obtained from XRD, DTA, TGA and four probe point method measurements for $(\text{Bi}_2\text{O}_3)_{1-x-y}(\text{Ho}_2\text{O}_3)_x(\text{Dy}_2\text{O}_3)_y$ ($x=1, 3, 5, 7, 9, 11$ mol%, $y=11, 9, 7, 5, 3, 1$ mol %) ternary system samples synthesized at different temperatures by solid state reaction method has been investigated in detail and some important results have been obtained for the chosen sample A6 as following:

- According to the obtained XRD results, all the samples synthesized at 700 °C, 750 °C and 800 °C for 48 hours have dominantly homogeneous face centered cubic $\delta\text{-Bi}_2\text{O}_3$ phase. The samples annealed at 650 °C have mixed phases composed from monoclinic $\alpha\text{-Bi}_2\text{O}_3$ phase and fcc $\delta\text{-Bi}_2\text{O}_3$ phase.
- According to conductivity measurements, all the samples, having stable $\delta\text{-Bi}_2\text{O}_3$ phase and synthesized at 700 °C, 750 °C, and 800 °C for 48 hours, have a good oxygen ion conductivity property.
- It has been observed that the electrical conductivity of all the samples increases while the percentage of the Ho_2O_3 doping materials increases.
- The best electrical conductivity has been observed for the sample A6 synthesized at 750 °C for 48 hours and having doping ratios % 11 mol for Ho_2O_3 and % 1 mol for Dy_2O_3 and maximum conductivity value has been measured as $6.11 \times 10^{-1} (\Omega \cdot \text{cm})^{-1}$.
- Stable δ -phase of $(\text{Bi}_2\text{O}_3)_{1-x-y}(\text{Ho}_2\text{O}_3)_x(\text{Dy}_2\text{O}_3)_y$ ternary system has been observed firstly in this study in operation conditions of an SOFC.

Comment

We are planning to perform resistance tests for this material for long time periods under the operation conditions to show that this material can be used as an electrolyte in SOFCs.

References

- [1] D. Music, S. Konstantinidis and J. M. Schneider, Equilibrium structure of $\delta\text{-Bi}_2\text{O}_3$ from first principle, *J. Phys.: Condens. Matter*, 21, 2009, 175403-175480.

- [2] C. -Y. Hsieh, K.-Z. Fung, Crystal structure and electrical conductivity of cubic fluorite-based $(\text{YO}_{1.5})_x(\text{WO}_3)_{0.15}(\text{BiO}_{1.5})_{0.85-x}$ ($0 \leq x \leq 0.4$) solid solutions, *J. Solid State Electrochem*, 13, 2009, 951-957.
- [3] P.K. Cheekatamarla, M. F. Caine, and J. Cai, Internal reforming of hydrocarbon fuels in tubular solid oxide fuel cells, *International Journal of Hydrogen Energy*, 33, 2008, 1853-1858.
- [4] S.R Xiao-Feng Ye, Z.R Wang, L. Wang, X.F Xiong, T.L. Sun Wen, Use of a catalyst layer for anode-supported SOFCs running on ethanol fuel, *Journal of Power Sources*, 177, 2008, 419-425.
- [5] M. Wang, and K. Woo, Impact of Sr_2MnO_4 preparation process on its electrical resistivity, *Energy Conversion and Management*, 49, 2008, 2409–2412.
- [6] S.H. Jung, E.D. Wachsman and N. Jiang, Structural Stability and Conductivity of Cubic $(\text{WO}_3)_x-(\text{Dy}_2\text{O}_3)_y-(\text{Bi}_2\text{O}_3)_{1-x-y}$, *International Journal of Ionics*, Volume 8, Numbers 3-4, 2002, 210-214.
- [7] M. Benkaddour, M.C. Steil, M. Drache, and P. Conflant, The Influence of Particle Size on Sintering and Conductivity of $\text{Bi}_{0.85}\text{Pr}_{0.105}\text{V}_{0.045}\text{O}_{1.545}$ Ceramics, *Journal of Solid State Chemistry*, 155, 2000, 273-279 .
- [8] N.M. Sammes, G.A. Tompsett, H. Nafe and F. Aldinger, Bismuth based oxide electrolytes structure and ionic conductivity, *Journal of European Ceramic Society*, 19, 1999, 1801-1826.
- [9] N. Jiang, E.D. Wachsman and S.H. Jung, A higher conductivity Bi_2O_3 -based electrolyte, *Solid State ionics*, 150, 3-4, 2002, 347-353.
- [10] H.A. Harwing, On the Structure of Bismuthsesquioxide: The α , β , γ , and δ -phase, *Z. Anorg. Allg. Chem.*, 444, 1978, 151-166.
- [11] A. Watanabe, Is it possible to stabilize $\delta\text{-Bi}_2\text{O}_3$ by an oxide additive?, *Solid State Ionics*, 40-41, 1990, 889-892 .
- [12] N. Jiang, R.M. Buchanan, F.E.G. Henn. A.F. Marshall, D.A. Stevenson, E.E. Wachsman, Aging phenomenon of stabilized bismuth oxides, *Mater. Res. Bull.*, 29, 1994, 247-254.
- [13] E.D. Wachsman, S. Boyapati, M.J. Kaufman, N. Jiang, Modeling of Ordered Structures of Phase-Stabilized Cubic Bismuth Oxides, *J. Am. Ceram. Soc.*, 83, 2000, 1964-1968.
- [14] E.D. Wachsman, G.R. Ball, N. Jiang and D.A. Stevenson, Structural and defect studies in solid oxide electrolytes, *Solid State Ionics*, 52, 1992, 213-218.
- [15] S. Boyabati, E.D. Wachsman and B.C. Chakoumakos, Neutron diffraction study of occupancy and positional oxygen ions in phase-stabilized cubic bismuth oxides, *Solid state Ionics*, 138, 2001, 293-304.